Gate Volume Estimation for Target Tracking*

Darko Mušicki
Dept of Electrical Engineering
University of Melbourne
Victoria 3010
Australia
d.musicki@ee.mu.oz.au

Mark R. Morelande
Dept of Electrical Engineering
University of Melbourne
Victoria 3010
Australia
m.morelande@ee.mu.oz.au

Abstract – *Gate volume is an integral part of many algorithms for non-parametric target tracking in clutter. Non-parametric target tracking assumes no a-priori knowledge of clutter measurement density. In the simplest case of a single-target single-state target tracking filter employing a Gaussian approximation, the gate is a hyper-ellipsoid whose volume can be calculated analytically. However, in a multi-target environment with closely spaced targets or in single target tracking with a mixture Gaussian approximation, the gate consists of overlapping hyper-ellipsoids and analytical evaluation of the gate volume is not possible. This paper presents a general algorithm for approximate estimation of volume of overlapping gates, together with tradeoffs between computing resources, volume estimation errors and its effects on target tracking performance.*

Keywords: target tracking, data association, gate calculation, false track discrimination, particle filters

1 Introduction

Data association algorithms deal with situations where there are measurements of uncertain origin. In many radar and sonar applications, for example, measurements (detections) originate not only from targets being tracked, but also from thermal noise as well as from various objects such as terrain, clouds etc. Unwanted measurements are usually termed clutter. Furthermore, true measurements from the target are present during each measurement scan with only a certain probability of detection, P_D. In a multi target situation, the measurements may have originated from one of several targets. Targets may also enter and leave the surveillance region at any time, so that at any given moment the number of targets in the surveillance area is unknown.

Optimal tracking in this environment requires one hypothesis for every possible measurement sequence to target assignment, including a null measurement to cater for the possibility that the target was not detected or that its measurement was not selected. Assuming that the measurement-target associations form a mutually exclusive and exhaustive set of events, as we will in this paper, the optimal filter cannot be implemented in practice as the number of hypotheses grows exponentially in time. Instead, various sub-optimal data association algorithms have been proposed. The most well-known of these methods is the probabilistic data association filter (PDAF) [4] which combines hypotheses from a single scan to produce a Gaussian approximation to the posterior distribution of the target state. The PDAF is surprisingly robust but tends to lose tracks once the clutter density increases above a certain level. Under these conditions a robust generalization of the PDAF in which association hypotheses from multiple scans are combined into a single Gaussian distribution [22] or a approximation of the posterior distribution by a Gaussian mixture [20] can be useful. Recently, particle filters have emerged as a potentially useful tool in target tracking. Particle filters approximate the posterior distribution of the target state by a set of random samples with associated weights [6]. The application of particle filters to target tracking problems has been investigated in, for instance, [1, 2, 8, 10, 11, 12, 13].

Gating, [3, 5] or measurement selection, is a necessary part of target tracking in clutter. The purpose of gating is to reduce computational expense by eliminating from consideration measurements which are far from the predicted measurement location. Gating is performed for each track at each scan by defining an area of surveillance space which is called the gate. All measurements positioned in the gate are selected and used for the track update while measurements not positioned in the gate are ignored for the purpose of the track update. The gate is usually formed in such a way that the probability of a target-originated measurement falling within the gate, provided that the target exists and is detected, is given by a gating probability P_G which can be evaluated from the available track statistics. Since the size or volume of the gate is dependent on the tracking accuracy it therefore varies from scan to scan and from track to track.

In many target tracking filters, the gate volume is used to measure clutter density which in turn is required to determine data association probabilities and the track quality measure. Computation of the gate volume is straightforward in the case of single target tracking filters which employ a Gaussian approximation, such as the PDAF. However, for single target tracking filters which approximate the posterior distribution by a Gaussian mixture or a set of particles, the gate is a union of overlapping hyper-ellipsoids. This applies even more generally to multi-target tracking

[1]This research has been supported by the Cooperative Research Centre for Sensor Signal and Information Processing under the Cooperative Research Centre scheme funded by The Commonwealth Government of Australia.

since, even if a Gaussian approximation is used, as in Joint PDAF (JPDAF) [3], the gating regions of targets in close proximity will overlap. Data association therefore requires computation of the volume of a region composed of several overlapping hyperellipsoids. No closed-form expression exists for this problem.

Several approaches have been suggested in the literature for overcoming this problem. In [3], the whole surveillance area was used in the derivation of the JPDAF. In [23], the volume of the overlapping hyperellipsoids was approximated by the volume of the largest individual gate. A similar approach was used in [9], except in that case the gating region was reduced to that of the largest individual gate. A Gaussian approximation was used to reduce the set of overlapping hyperellipsoids to a single hyperellipsoid in [24]. In all of the cited examples no attempt was made to estimate the volume of the actual gate. To the best of the authors' knowledge, the only attempt to estimate the volume of the overlapping ellipsoid gate was made in [15] where the number of measurements shared between gates was used as a measure of overlap between gates. In this paper we consider two methods for estimating the gate volume. The first is a naive Monte Carlo estimator which generates samples in a region bounding the gate and counts the proportion of samples falling within the gate. The second is based on the approach of [15]. The main difference is that we use not only existing measurements but also additional randomly generated points to to increase estimation accuracy of the overlap. This is seen to be particularly important in particle filter implementations. The performances of the two gate volume estimators are compared for a simple example.

The paper layout is as follows. Section 2 presents a brief overview of simple and complex gating schemes. The gate volume estimators are presented and compared in Section 3. Simulation results evaluating the performance of the overlap volume estimator in terms of its effect on tracking performance are given in Section 4. Two examples are considered. The first is single target tracking in clutter using a particle filter. The second is multi-target tracking using the JPDAF. Conclusions are drawn in Section 5.

2 Gating

For each track, gating involves finding a minimum volume of space which contains the target measurements, (conditioned on the target existence and detection) with a given probability P_G. The main objective is to reduce the size of the measurement set that the tracking filter needs to process and thus to limit computational requirements. In a non-uniform clutter environment a fringe benefit of gating is to limit the clutter measurement density fluctuations within the gate.

The use of gate volume in data association and track quality evaluation can be illustrated using the integrated PDAF (IPDAF) [18]. The probability of target existence update and data association probabilities are computed using:

$$\delta_k = \begin{cases} P_D P_G \left(1 - \frac{V_k}{\hat{m}_k} \sum_{j=1}^{m_k} p_j\right); & m_k > 0 \\ P_D P_G; & m_k = 0 \end{cases} \quad (1)$$

$$\psi_{k|k} = (1-\delta_k)\psi_{k|k-1}/(1-\delta_k\psi_{k|k-1}) \quad (2)$$

$$\beta_{k,j} = \begin{cases} (1-P_D P_G)/(1-\delta_k); & j=0, \\ P_D P_G \hat{\lambda}_k p_i/(1-\delta_k); & j=1,\ldots,m_k \end{cases} \quad (3)$$

where, at scan k, V_k denotes the gate volume, m_k denotes the number of validated measurements, $\hat{m}_k$ denotes the expected number of selected clutter measurements, p_j denotes a-priori probability density function (pdf) of measurement j, $\psi_{k|k-1}$ and $\psi_{k|k}$ denote the a-priori and a-posteriori probability of target existence respectively, and $\beta_{k,0}$ and $\beta_{k,j}$ denote data association probabilities of the null measurement and measurement j respectively. Gate volume is used in a similar fashion by other target tracking algorithms.

Since the IPDAF commonly employs a Gaussian approximation, the IPDAF gate is a single hyper-ellipsoid. For measurements $z_k \in \mathbb{R}^{n_z}$, assume that the a-priori measurement pdf of a track can be described by a Gaussian pdf $p(z_k|z^{k-1}) = N(z_k; \hat{z}_k, S_k)$, where

$$N(z;\mu,\Sigma) = \exp\{-(z-\mu)'\Sigma^{-1}(z-\mu)/2\} \Big/ \sqrt{|2\pi\Sigma|}$$

and $z^{k-1} = (z_1,\ldots,z_{k-1})$ denotes the measurement history to time $k-1$. The gating region G is then defined as

$$G = \{z \in \mathbb{R}^{n_z} | \, (z-\hat{z}_k)' \, S_k^{-1} \, (z-\hat{z}_k) \leq g^2\} \quad (4)$$

and the gate volume is given by

$$V_k = c\,(n_z) \left|g^2 S_k\right|^{1/2} \quad (5)$$

where $c(n_z) = \pi^{n_z/2}/\Gamma(n_z/2+1)$ is the volume of a unit radius n_z-dimensional unit hypersphere [3]. The simple gate, as defined by (4) and (5) is used by a class of single-target tracking filters based on PDA; eg. PDAF [4] and IPDAF [18]. The threshold g^2 is selected in order to give a specified gating probability P_G [4].

In general however, the gate may consist of union of overlapping simple gates, which we call the complex gate, i.e., we consider a gating region

$$G = \bigcup_{i=1}^{n} G_i \quad (6)$$

where G_i, $i = 1,\ldots,n$ is a gate of the type shown in (4). If, $G_{i_1} \cup G_{i_2} \neq \emptyset$, i.e., there is overlap between individual gates, then

$$V_G \neq \sum_{i=1}^{n} V_{G_i}$$

where V_A denotes the volume contained in the region of space defined by A. In such cases the volume V_G of a complex gate cannot be found in closed-form. This is a common occurrence in the following scenarios:

• the track consists of a number of components and each component creates a simple gate; eg. integrated track split (ITS) filter [17], particle filter [13],

• the tracker includes multiple model based estimation algorithm in order to track maneuvering targets, and each model creates a simple gate, eg. IPDA-IMM [14, 24],

• multi-target tracking filter based tracks share selected measurement(s), in which case the complex gate is called the cluster; eg. JPDAF [3], joint IPDAF (JIPDAF) [15],

• A combination of the above.

The complex gate can be a union of identical simple gates, eg. particle filter based target tracking algorithms, similarly sized simple gates, eg. ITS, or very differently sized simple gates, eg. JIPDA. The number of simple gates varies from relatively few, eg. JIPDA, to the order of tens, eg. ITS, to the order of hundreds, eg. particle filter.

3 Gate Volume Estimation

The gating region G is assumed to be composed of n possibly overlapping regions $G_1, \ldots, G_n$ as shown in (6). As discussed above, accurate estimation of the volume V_G of the gating region is required for target tracking. Two possible estimators will be presented and compared in the following sections.

3.1 Naive Monte Carlo estimation

We consider first a simple Monte Carlo (MC) volume estimator. Let B denote the region of measurement space occupied by the smallest hyper-rectangle for which $G_i \subset B$, $i = 1, \ldots, n$. The volume of B is denoted as V_B. The naive Monte Carlo estimator places random samples uniformly in B and estimates V_G by the proportion of samples which fall inside G. The volume of G can then be estimated as

$$\hat{V}_G = \frac{V_B}{s} \sum_{t=1}^{s} \chi_G(u_t) \tag{7}$$

where $u_t \sim U_B$, $t = 1, \ldots, s$ with U_B denoting the density of a random variable uniformly distributed over B, i.e., $U_B(z) = \chi_B(z)/V_B$ and $\chi_A(z) = 1$ if $z \in A$ and zero otherwise and s denotes the number of random samples.

It is shown in Appendix A that $\mathsf{E}\,\hat{V}_G = V_G$ and $\mathrm{var}(\hat{V}_G) = V_G(V_B - V_G)/s$ so that $\hat{V}_G$ is and unbiased and consistent (in the number s of Monte Carlo realisations) estimator of V. The variance expression is intuitively appealing since it confirms the obvious supposition that the accuracy of the estimator should improve as the bounding region B provides a closer approximation to the gating region G.

3.2 Overlap Monte Carlo estimator

The second estimator, first proposed in [15], takes advantage of the particulate nature of the gating region. Since we know the volume of each individual gate the unknown factor required for determination of the total gate volume is the amount of overlap between the individual gates. Overlap can be estimated by placing samples in the gating region and noting the number of individual gates which contain each sample. This results in the estimator

$$\tilde{V}_G = \sum_{i=1}^{n} V_{G(i)} \sum_{t=1}^{s} \chi_G(u_t) \Bigg/ \sum_{t=1}^{s} \sum_{i=1}^{n} \chi_{G(i)}(u_t) \tag{8}$$

where $G(i), i = 1, \ldots, n$ denotes the simple gate i. If s is small, as would be desired in practice, and the volume of one of the individual gates far exceeds that of the others, it may be necessary to use the modified estimator $\max(V_{\max}, \tilde{V}_G)$ where

$$V_{\max} = \max_{i=1,\ldots,n} V_{G(i)} \tag{9}$$

Note that the samples $u_1, \ldots, u_s$ need not all be artificially generated since, if the clutter is uniformly distributed, existing measurements can be used as in [15]. This approach has produced good results although it should be kept in mind that the measurement set also contains a target measurement which is not uniformly distributed.

3.3 Comparison of the volume estimators

A simple test case is used to give an idea of the behaviour of the two volume estimators. We consider a 2-dimensional measurement space in which the gating region is composed of two circular regions. One circle is located, in Cartesian coordinates, at $(5, 5)$ and has radius 5. The location and radius are varied in order to examine the properties of the two estimators.

In the first experiment the radius of the second gate is fixed to 5, the same as that of the first circle, and the gate is centred at $(x, 5)$ with x varied between 5 and 15. Note that $x = 5$ corresponds to complete overlap and $x = 15$ corresponds to zero overlap. The variances of the volume estimators for $s = 25$ are estimated using 10 000 realisations for each value of x. Note that although an expression for the variance of $\hat{V}_G$ has been derived it cannot be used for our present purposes as it depends on the unknown value of V_G. The estimated standard deviations normalised by the gate volume are plotted against x-position in Figure 1. The superior accuracy of $\tilde{V}_G$ compared to $\hat{V}_G$ is clearly evident, particularly when there is large amount of overlap between the circular regions or when there is almost no overlap. The behaviour of $\hat{V}_G$ confirms the analysis of Appendix A which gives the normalised standard deviation of $\hat{V}_k$ as

$$\mathrm{std}(\hat{V}_G)/V_G = \sqrt{(V_B/V_G - 1)/s} \tag{10}$$

In the current example, it can be verified that the ratio V_B/V_G is minimised for $x = 10$ and increases monotonically with $|x - 10|$. This gives rise to the curve shown in Figure 1.

In the second experiment the location of the centre of the second gate is fixed at (5,10) and the radius is varied between 0 and 10. For each radius, 10 000 realisations are used to estimate the variances of the volume estimators. The results are shown in Figure 2. Once again the overlap MC estimator is seen to be superior to the naive MC estimator. The normalised standard deviation of the naive

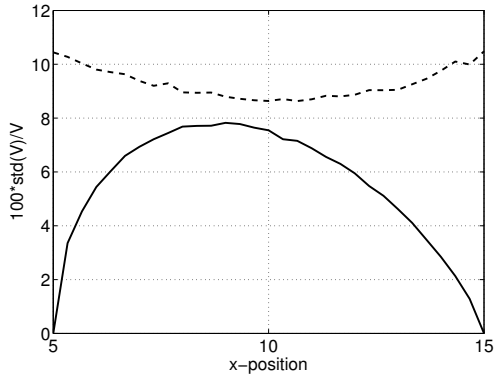

Fig. 1: Normalised standard deviation of the naive estimator (dashed) and the overlap estimator (solid) plotted against the x-position of the second gate. The first gate is at $x = 5$. Both gates have radius 5.

MC estimator approaches that of the overlap MC estimator when the radii of the two gating regions are approximately equal. However, when the radii of the two gates are considerably different the overlap MC estimator is significantly more accurate than the naive MC estimator. As shown in (10), the behaviour of the naive MC estimator is a direct result of the variations of V_B/V_G with the radius of the second gate.

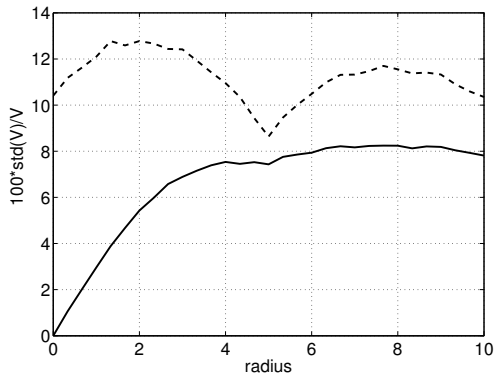

Fig. 2: Normalised standard deviation of the naive estimator (dashed) and the overlap estimator (solid) plotted against the radius of the second gate. The first gate has radius 5. Both gates are centred at (5,5).

The superior performance of the overlap estimator can be attributed to the fact that this estimator uses the available information on the structure of the gating region and the volume of the individual gates. By not using this information the naive volume estimator sacrifices performance for generality.

4 Simulation Study

4.1 Volume estimation for particle filtering

A useful application of the volume estimators proposed in Section 3 is in target tracking using particle filters. The issue of developing appropriate windowing methods for target tracking using particle filtering has not been addressed in the literature. In [13] windows of constant radius were used. This is not ideal since the window dimensions must be chosen to give approximately unity gating probability at all times. This results in the gate being larger than necessary for much of the time. The method proposed here modifies the gate size according to the tracking accuracy therefore decreasing the number of validated measurements. The use of the volume estimation techniques in particle filtering is demonstrated in the following scenario involving nonlinear target measurements and clutter.

Consider a target moving in the plane with state $x_k = (\xi_k, \dot{\xi}_k, \zeta_k, \dot{\zeta}_k)' \in \mathbb{R}^4$, where ξ_k and ζ_k denote, respectively, x and y position, which evolves according to the stochastic difference equation

$$x_k = Fx_{k-1} + v_k, \qquad k = 1, 2, \ldots, \tag{11}$$

where $\{v_k \sim N(0, Q)\}$ is white and

$$F = I_2 \otimes \begin{pmatrix} 1 & T \\ 0 & 1 \end{pmatrix} \tag{12}$$

with I_p denoting the $p \times p$ identity matrix, $\otimes$ denoting the Kronecker product and T denoting the sampling period. The initial state $x_0 \sim \pi_0$ is independent of $\{v_k\}$. At each time step a collection of m_k measurements $z_k = \{z_{k,1}, \ldots, z_{k,m_k}\}$ containing clutter measurements and, if detected, a target measurement is obtained. Association hypotheses $\theta_{k,0}, \ldots, \theta_{k,m_k}$ define the origin of each measurement. Under $\theta_{k,j}$, $j \in \{1, \ldots, m_k\}$ the jth measurement originates from the target and satisfies, for $k = 1, 2, \ldots$,

$$\begin{aligned} z_{k,j} &= h(x_k) + e_k \\ &= \begin{pmatrix} \sqrt{\xi_k^2 + \zeta_k^2} \\ \arctan(\zeta_k/\xi_k) + \pi\chi_{(-\infty,0)}(\xi_k) \end{pmatrix} + e_k, \end{aligned} \tag{13}$$

where $\{e_k \sim N(0, R)\}$ is white and independent of $\{v_k\}$ and x_0. The remaining measurements are due to clutter which is uniformly distributed in the measurement space with the number of clutter points falling in a region of volume V assumed to follow a Poisson distribution with unknown mean λV. Under $\theta_{k,0}$ all measurements are due to clutter.

We now develop a particle filter for target tracking in the scenario described above. We use a simple implementation, the bootstrap filter [7], since our focus is on demonstrating the usefulness of the volume estimation techniques. The volume estimators are also applicable to more sophisticated techniques, the use of which would provide improved performance with significant improvements under some conditions.

Assume that the posterior distribution at time $k-1$ is represented by a set of particles $x_{k-1}^1, \ldots, x_{k-1}^n$ with weights $w_{k-1}^1, \ldots, w_{k-1}^n$. The bootstrap filter first predicts forward each particle by simulating the stochastic difference equation which the target dynamics are assumed to obey:

$$x_k^i \sim N(Fx_{k-1}^i, Q), \quad i = 1, \ldots, n. \tag{14}$$

The particle weights are then updated using the likelihood. This is where the windowing procedure is used to reduce

the computational load of the algorithm. The location of the predicted target measurement obeys

$$p(z_k|z^{k-1}) = \int p(z_k|x_k)p(x_k|z^{k-1})\,dx_k = \sum_{i=1}^{n} w_{k-1}^i N(z_k; h(x_k^i), R) \quad (15)$$

The gate is therefore given by (6) with

$$G_i = \{z \in \Omega_z | (z - h(x_k^i))' R^{-1} (z - h(x_k^i)) < g^2\} \quad (16)$$

where $\Omega_z = [0, \infty) \times [-\pi, \pi)$ and g^2 is determined by the pre-defined gating probability P_G [4]. Let

$$J = \{j \in \{1, \ldots, m_k\} | z_{k,j} \in G\} \quad (17)$$

denote the indices of the validated measurements and l_k denote the number of validated measurements. The weight update can then be computed as, for $i = 1, \ldots, n$,

$$w_k^i = w_{k-1}^i \psi_k^i \Big/ \sum_{t=1}^{n} w_{k-1}^t \psi_k^t \quad (18)$$

where

$$\psi_k^i = 1 - P_D P_G + \frac{P_D P_G \tilde{V}_k}{l_k - P_D P_G} \sum_{j \in J} N(z_{k,j}; h(x_k^i), R) \quad (19)$$

with $\tilde{V}_k$ denoting the overlap gate volume estimator of (8). Note that we consider only the overlap volume estimator for reasons demonstrated in Section 3.3.

It is also necessary to perform resampling of the particle set every few scans [7]. In the simplest terms, this involves removing insignificantly weighted particles by sampling with replacement from the particle set according to the particle weights. Resampling prevents the occurrence of sample degeneracy.

A simple alternative to the gating scheme used here is to apply a Gaussian approximation to (15), in the spirit of [24]. It is worthwhile examining the performance of this approximation as it is computationally simpler, in terms of both gating and gate volume computation, than an approach based on n individual gates. Approximating (15) by a Gaussian distribution with the same mean and covariance matrix gives

$$\hat{p}(z_k|z^{k-1}) = N(z_k; \hat{z}_k, \hat{S}_k) \quad (20)$$

where

$$\hat{z}_k = \sum_{i=1}^{n} w_{k-1}^i h(x_k^i) \quad (21)$$

$$\hat{S}_k = R + \sum_{i=1}^{n} w_{k-1}^i h(x_k^i) h(x_k^i)' - \hat{z}_k \hat{z}_k' \quad (22)$$

A simple gating scheme can then be used to find validated measurements, compute the gate volume and compute the likelihood as in (19). This scheme will be referred to as the Gaussian gating scheme. As a useful benchmark, we also consider the performance of the standard tracking algorithm the PDA-EKF which follows the formulation of [4] with the Kalman filter recursion replaced by an extended Kalman filter recursion.

Track loss percentages are used to assess the competing algorithms. A target track is deemed lost if, in five consecutive scans, the error in the estimated target position exceeds a threshold. Two sets of simulations are considered. In the first set of simulations we investigate the effect on tracking performance of the gate volume estimation accuracy. The second set of simulations compares the proposed gating method with the Gaussian gating method as a function of the number of particles. The model parameters are as follows for both sets of simulations. The distribution of the initial target state is $\pi_0 = N(\hat{x}_0, P_0)$ with

$$\hat{x}_0 = (75, -5, 75, 8)'$$
$$P_0 = \text{diag}(100, 5, 100, 5) \quad (23)$$

The process noise and measurement noise covariance matrices are set to

$$Q = I_2 \otimes q \begin{pmatrix} T^3/3 & T^2/2 \\ T^2/2 & T \end{pmatrix} \quad (24)$$

$$R = \text{diag}(25, (\pi/180)^2) \quad (25)$$

with $q = 1/8$. The clutter density is set to $\lambda = 1/6/(\text{m} \cdot \text{rad})$. The detection probability $P_D = 0.7$ and the gating probability $P_G = 0.9999$. For each set of parameters used here, 2500 realisations of length 60 time steps are used to compute track loss percentages.

Figures 3 and 4 shows the track loss percentage of the bootstrap filter using the proposed gating scheme with gate volume estimated using the overlap method plotted against the number s of MC realisations. Figure 3 shows results for $n = 200$ particles and Figure 4 shows results for $n = 500$ particles. The performances of the bootstrap filter with the Gaussian gating method and the PDA-EKF are also shown. It appears that, in this example, selecting $s = 20$ provides a reasonable trade-off between computational efficiency and performance as only small decreases in the track loss percentage are achieved by using larger values of s. As few as $s = 10$ MC realisations suffice for the proposed gating scheme to outperform the Gaussian gating scheme. It is reassuring to find that the required value of s is seemingly independent of the number of particles. Trials with a larger number of particles would be required to verify this.

Track loss percentages for bootstrap filtering with the proposed gating scheme and the Gaussian approximation scheme are plotted against the number n of particles in Figure 5. 50 MC realisations are used to estimate the gate volume in the proposed gating scheme. There are two points of interest. Firstly, it is clear that, for any given number of particles, the proposed gating scheme outperforms the Gaussian gating scheme. Secondly, the performance of the Gaussian gating scheme does not approach that of the proposed gating scheme as n increases. In fact, the difference between the performances of the two algorithms seems to increase slightly as n increases. These improvements can be attributed to the fact that the proposed gating scheme

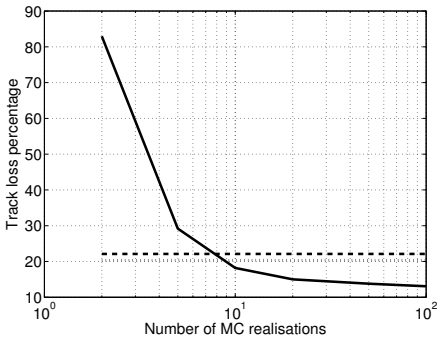

Fig. 3: Track loss percentage of bootstrap filter with proposed gating scheme (solid) plotted against number of MC realisations used in gate volume estimation. Results are shown for $n = 200$ particles. The performances of the PDA-EKF and bootstrap filter with Gaussian gating scheme are indicated by a dotted line and dashed line, respectively.

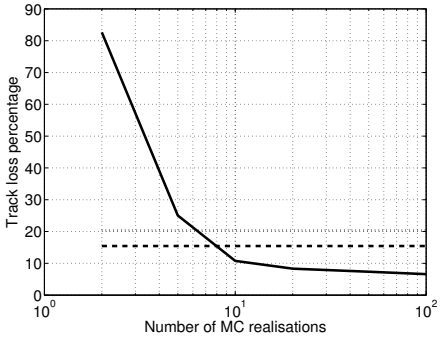

Fig. 4: Track loss percentage of bootstrap filter with proposed gating scheme plotted against number of MC realisations used in gate volume estimation. Results are shown for $n = 500$ particles. The performances of the PDA-EKF and bootstrap filter with Gaussian gating scheme are indicated by a dotted line and dashed line, respectively.

mirrors the multi-modal nature of the posterior distribution. The Gaussian gating scheme tends to ignore modes which are distant from the predicted measurement location.

The improved performance of the proposed gating scheme compared to the Gaussian gating scheme comes at the expense of a significantly larger number of computations. In the current example, the bootstrap filter with the proposed gating scheme has about 1.4 times the computational expense of the bootstrap filter with the Gaussian gating scheme. The main computational expense of the proposed gating method seems to be incurred in deciding which gates a each measurement belongs to. A possible direction for future research is to look at reducing this expense by looking at approximate, computationally simple methods of deciding whether a particular point in space is enclosed by a given hyperellipsoid.

4.2 Multi-target tracking using the JPDAF

We consider r targets with state of the ith target denoted as $x_{i,k}$, $i = 1, \ldots, r$. The target states satisfy the stochastic

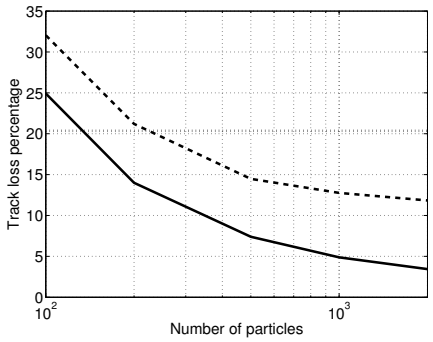

Fig. 5: Track loss percentage of bootstrap filter with proposed gating scheme (solid) and Gaussian gating scheme (dashed) plotted against number of particles. $s = 50$ realizations are used to estimate the gate volume. The performance of the PDA-EKF is indicated by a dotted line.

difference equations

$$x_{i,k} = F x_{i,k-1} + v_{i,k}, \qquad k = 1, 2, \ldots,$$

where F is given in (12) and $\{v_{i,k} \sim N(0, Q_i)\}$ are white and mutually independent. The initial states $x_{i,0} \sim \pi_{i,0}$ are independent of the processes $\{v_{i,k}\}$. Measurements of target position are made in Cartesian coordinates with measurement noise $\{e_k \sim N(0, R)\}$ independent of $\{v_{i,k}\}$ and $x_{i,0}$, $i = 1, \ldots, r$. The clutter assumptions are the same as Section 4.1.

The JPDAF, formulated in [3], can be used to obtain estimates of the state of each target. Since the JPDAF approximates the posterior distribution of each target state by a Gaussian distribution, the gating region is comprised of r hyperellipsoids, one for each target. A complex gating scheme arises only when the targets are sufficiently close for some of the individual gates to overlap. In this set of simulations we examine the use of the overlap gate volume estimator in such situations. The particular scenario under consideration contains $r = 3$ targets. The initial target states are $x_{i,0} \sim N(\hat{x}_{i,0}, P_0)$, $i = 1, 2, 3$ where

$$\hat{x}_{i,0} = (100, 10, 450 - 25ui, 2u - ui)'$$
$$P_0 = I_2 \otimes 25 \begin{pmatrix} 1 & 1 \\ 1 & 2 \end{pmatrix}$$

The parameter u is referred to as the relative target velocity in the y-direction. This controls the amount of time the targets are in close proximity with small values of u resulting in the targets being close for a large amount of time. Note that, in the absence of process noise, this model results in the targets meeting at time $k = 25$. The addition of Gaussian process noise with covariance matrix given by (24) with $q = 1/200$ will slightly modify the location of this crossing point. The measurement noise covariance matrix is $R = 25I_2$. The detection probability $P_D = 0.8$ and the gating probability $P_G = 0.999$. The clutter density is set to $\lambda = 1 \times 10^{-4}/\mathrm{m}^2$. As in the Section 4.1 performance is assessed using the percentage of tracks lost as a performance metric.

Table 1: Track loss percentages for the JPDAF using the proposed gating scheme with $\bar{s}$ additional MC realisations used to estimate the gate volume.

$\bar{s}$	Relative target velocity u		
	3	4	5
0	15.8	16.6	16.6
5	16.6	16.6	16.6
10	16.6	16.2	16.6

The gate volume is estimated using (8) with existing measurements used in addition to uniformly generated samples. The number of additional samples generated is denoted as $\bar{s}$. Note that the use of existing measurements inevitably results in target-originated measurements being used in gate volume estimation since there is no way to distinguish between clutter and target measurements. Table 1 shows the track loss percentages for various values of relative velocity u and $\bar{s}$. Note that $\bar{s} = 0$ corresponds to gate volume estimation using only existing measurements. 500 realisations of 50 time steps each were used to generate these results. The results show that the generation of uniformly distributed samples for gate volume estimation is unnecessary as sufficient volume estimation accuracy can be obtained from the existing measurements. For the clutter density used here there are usually one, sometimes two, clutter measurements in an individual target gate. This is considerably different from the situation encountered in Section 4.1 where it was demonstrated that, for single target tracking using a particle filter, performance improves significantly as the number s of MC realisations used in the gate volume estimation is increased from 1 to 20. For $s > 20$, performance improvements are not as dramatic but are still appreciable. The difference in behaviour between the two examples can be attributed to the vastly different numbers of individual gates comprising the gating region in each case. In the case of multi-target tracking using the JPDAF there are at most three hyperellipsoids in the present example while in the particle filtering example there are typically hundreds of hyperellipsoids. This increased number of hyperellipsoids greatly increases the complexity of the gating region therefore necessitating the use of a larger number of MC realisations in the gate volume estimation.

5 Conclusions

Measurement selection or gating is an integral part of the vast majority of target tracking algorithms. The volume of the selection space or gate is part of data association and track quality calculations. However, except for a class of single-target, single scan, non- maneuvering target tracking filters, the exact formula for gate volume calculation does not exist in a closed form.

An efficient approximation for complex gate volume is presented in this paper, as well as complexity/tracking filter capabilities tradeoff. Approximation of the gate volume is performed using a Monte Carlo approximation. In the context of single target tracking in clutter using a particle filter it was shown that good performance can be obtained using a relatively small number of Monte Carlo realisations. For multi-target tracking using the joint probabilistic data association filter it was shown that, in the given example, gate volume estimation can be performed using the existing data. The use of additional Monte Carlo realisations provides no improvement in tracking performance.

A Properties of naive Monte Carlo estimator

The expectation of the naive Monte Carlo estimator can be written as

$$\mathsf{E}\hat{V}_G = V_B/s \sum_{t=1}^{s} \int \chi_G(u_t) \prod_{j=1}^{s} \{\chi_B(u_j)\, du_j/V_B\} \quad (26)$$

Since

$$\int \chi_G(u_t)\chi_B(u_j)\, du_j = \begin{cases} V_B;\ j \neq t \\ V_G;\ j = t \end{cases} \quad (27)$$

we have

$$\begin{aligned} \mathsf{E}\hat{V}_G &= V_B/s \sum_{t=1}^{s} V_G V_B^{s-1}/V_B^s \\ &= V_G \end{aligned} \quad (28)$$

as required.

The second-order moment of $\hat{V}_G$ is

$$\begin{aligned} E(\hat{V}_G)^2 = V_B^2/s^2 \sum_{t_1=1}^{s}\sum_{t_2=1}^{s} \int \chi_G(u_{t_1})\chi_G(u_{t_2}) \\ \times \prod_{j=1}^{s} \{\chi_B(u_j)\, du_j/V_B\} \end{aligned} \quad (29)$$

Eq. (29) is composed of s terms of the form

$$\int \chi_G(u_t) \prod_{j=1}^{s} \{\chi_B(u_j)\, du_j\} = V_G V_B^{s-1} \quad (30)$$

and $s(s-1)$ terms of the form

$$\int \chi_G(u_{t_1})\chi_G(u_{t_2}) \prod_{j=1}^{s} \{\chi_B(u_j)\, du_j\} = V_G^2 V_B^{s-2} \quad (31)$$

Substituting into (29) gives

$$\begin{aligned} \mathsf{E}(\hat{V}_G)^2 &= V_B^2/s^2 \left(sV_G/V_B + s(s-1)V_G^2/V_B^2\right) \\ &= V_G^2 + V_G(V_B - V_G)/s \end{aligned} \quad (32)$$

The variance of $\hat{V}_G$ is then found as

$$\mathrm{var}(\hat{V}_G) = \mathsf{E}(\hat{V}_G)^2 - (\mathsf{E}\hat{V}_G)^2 = V_G(V_B - V_G)/s \quad (33)$$

References

[1] M.S. Arulampalam, S. Maskell, N. Gordon, and T. Clapp. A tutorial on particle filters for online nonlinear/non-Gaussian Bayesian tracking. *IEEE Transactions on Signal Processing*, 50(2):174–188, 2002.

[2] D. Avitzour. Stochastic simulation Bayesian approach to multitarget tracking. *IEE Proceedings F.- Radar, Sonar and Navigation*, 142(2):41–44, 1995.

[3] Y. Bar-Shalom and T. E. Fortmann. *Tracking and Data Association*. Academic Press, 1988.

[4] Y. Bar-Shalom and E. Tse. Tracking in a cluttered environment with probabilistic data association. *Automatica*, 11:451–460, 1975.

[5] S. Blackman and R. Popoli. *Design and Analysis of Modern Tracking Systems*. Artech House, 1999.

[6] A. Doucet, S. Godsill and C. Andrieu. On sequential Monte Carlo sampling methods for Bayesian filtering. in *Statistics and Computing*, 10:197–208, 2000.

[7] N.J. Gordon, D.J. Salmond, and A.F.M. Smith. Novel approach to nonlinear/non-Gaussian Bayesian state estimation. *IEE Proceedings-F*, 140(2):107–113, 1993.

[8] F. Gustafsson, F. Gunnarsson, N. Bergman, U. Forssell, J. Jansson, R. Karlsson and P.-J. Nordlund. Particle filters for positioning, navigation and tracking. In *IEEE Transactions on Signal Processing*, 50(2):425–437, 2002.

[9] A. Houles and Y. Bar-Shalom. Multisensor tracking of a maneuvering target in clutter. In *IEEE Transactions on Aerospace and Electronic Systems*, 25(2):176–189, 1989.

[10] R. Karlsson and N. Bergman. Auxiliary particle filters for tracking a manoeuvring target. In *Proceedings of the IEEE Conference on Decision and Control*, pages 3891–3895, 2000.

[11] R. Karlsson and F. Gustafsson. Range estimation using angle-only target tracking with particle filters. In *Proceedings of the American Control Conference*, pages 3743–3748, Arlington, USA, June, 2001.

[12] S. McGinnity and G.W. Irwin. Manoeuvring target tracking using a multiple-model bootstrap filter. In *Sequential Monte Carlo Methods in Practice*, Springer-Verlag, New York, 2001.

[13] M.R. Morelande, S. Challa, and N. Gordon. A study of the application of particle filters to single target tracking problems. In *Proceedings of the SPIE*, volume 5204, 2003.

[14] D. Mušicki, S. Challa and S. Suvorova. Automatic Track Initiation for Tracking of Maneuvering Target in Clutter. In *ASCC 2004, submitted*, Melbourne, Australia, 2004.

[15] D. Mušicki and R. J. Evans. Joint Integrated Probabilistic Data Association - JIPDA. In *Fusion 2002 Conference*, Annapolis, Maryland, 2002.

[16] D. Mušicki, R. J. Evans, and B. F. La Scala. Multi-scan parametric target tracking in clutter. In *42nd IEEE Conference on Decision and Control*, Maui USA, December 2003.

[17] D. Mušicki, R. J. Evans, and B. F. La Scala. Integrated tracking splitting suite of target tracking filters. In *6th International Conference on Information Fusion*, pages 1039–1046, Cairns Australia, July 2003.

[18] D. Mušicki, R. J. Evans, and S. Stanković. Integrated probabilistic data association. *IEEE Transactions on Automatic Control*, 39(6):1237–1241, 1994.

[19] D. B. Reid. An algorithm for tracking multiple targets. *IEEE Transactions on Automatic Control*, 24:843–854, 1979.

[20] D.J. Salmond. Mixture reduction algorithms for target tracking. In *Proceedings of the IEE Colloquium on State Estimation in Aerospace and Tracking Algorithms*, pages 7/1–7/4, 1989.

[21] B. F. La Scala and G. W. Pulford. Viterbi data association tracking for Over-The-Horizon Radar. In *International Radar Symposium*, pages 1155–1164, Munich, Germany, 1998.

[22] R.A. Singer, R.G. Sea, and K.B. Housewright. Derivation and evaluation of improved tracking filters for use in dense multitarget environments. *IEEE Transactions on Information Theory*, 20(4):423–432, 1974.

[23] G.W. Pulford and R.J. Evans. A multipath data association tracker for over-the-horizon radar. In *IEEE Transactions on Aerospace and Electronic Systems*, 34(4):1165–1183, 1998.

[24] X. Wang, S. Challa, and R. J. Evans. Gating techniques for maneuvering target tracking in clutter. *IEEE Transactions on Aerospace and Electronic Systems*, 38(3):1087–1097, July 2002.